Summary: Clay/PMMA nanocomposites were prepared by melt blending of an organically modified MMT with PMMA under various process conditions. The MMT clay was initially cation exchanged with octadecylammonium to enhance its hydrophobicity and to expand the interlamellar space of the silicate plates. PMMA was then inserted into the inter-lamellar space of the modified clay by melt blending at an elevated temperature. The effects of blending temperature, blending time, and clay/PMMA compositions on the level of expansion and homogenization were investigated. Composites with intercalated and/or exfoliated clay structure were obtained depending upon the process conditions, as confirmed by XRD diffractometry. The thermal decomposition temperature (T_d) and glass transition temperature (T_g) of the composites were determined, respectively, by TGA and DSC analyses. Marked improvements, up to 35 °C, of the thermal stability (T_d) with respect to pure PMMA were achieved for many of the composite samples. The T_g of the composites, however, does not increase accordingly. Furthermore, a novel type of bone cement was synthesized by applying the clay/PMMA nanocomposites as a substitute for PMMA in a typical formulation. These bone cements demonstrated much higher impact strength and better cell compatibility than the surgical Simplex P cement. Therefore, the bone cements with clay/PMMA nanocomposites meet the requirement for the architectural design of orthopedic surgery.

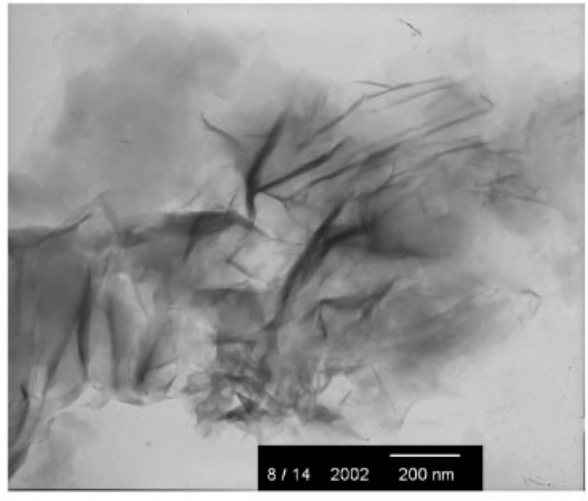

TEM images of an OA-clay/PMMA composite.

Preparation of Clay/PMMA Nanocomposites with Intercalated or Exfoliated Structure for Bone Cement Synthesis

Jyh-Horng Wang,[1] *Tai-Horng Young,*[2] *Dar-Jong Lin,*[3] *Min-Kuei Sun,*[3] *Han-Shiang Huag,*[3] *Liao-Ping Cheng**[3]

[1] Department of Orthopedic Surgery, National Taiwan University Hospital, Taipei 10016, Taiwan
[2] Institute of Biomedical Engineering, College of Medicine and College of Engineering, National Taiwan University, Taipei 10016, Taiwan
[3] Department of Chemical and Materials Engineering, Tamkang University, Taipei 25137, Taiwan
E-mail: lpcheng@mail.tku.edu.tw

Received: November 24, 2005; Revised: February 27, 2006; Accepted: March 1, 2006; DOI: 10.1002/mame.200500389

Keywords: bone cement; cell culture; clay; intercalation; nanocomposites

Introduction

Clay/polymer nanocomposite is a novel type of organic/inorganic composite material, which attracts a great deal of attention in recent years as a reinforcing material superior to its conventional counterpart, viz., blends with micron-scale phase domains.[1–23] While several useful materials of this kind have been commercialized, such as mica-Nylon 6 (Unitika Ltd., Japan) and organo-modified clay/poly(propylene) (Nanocor Inc., China), considerable research activities are still undergoing in various aspects, such as developments of new materials with unique properties, synthesis process being cost effective and environmental friendly, and new applications to satisfy specific needs. To prepare this new type of composite, clay minerals, e.g., mica, montmorillonite (MMT), bentonite, etc., are processed to disperse in a polymer matrix such that the silicate lamellae in the clay are expanded and randomized by the

insertion action of entangled polymer chains. As nanoscale mixing is established, interactions between organic and inorganic components become strong through extensive interfacial contacts. Thereby, thermal and mechanical properties of the polymer can easily be enhanced by just a small dosage of clay (typically <5%). In addition, functionalized polymers can be introduced to provide the synthesized composites with specific properties (optical, electrical, biocompatible, etc.).

In the present research, nanocomposites of MMT/poly(methyl methacrylate) (PMMA) were prepared by a melt blending process, in which PMMA was intercalated into the inter-lamellar space of an organically modified MMT at an elevated temperature.[14,15] Depending on the preparation conditions, such as blending temperature, blending time, and clay content, different degrees of intercalation and in many cases exfoliation of the clay could be obtained. A variety of clay/PMMA nanocomposites have been prepared using different types of intercalation agents, clays, or synthesis techniques as reported in the recent literature.[14–23] For example, Okamoto used in situ intercalative polymerization of methyl methacrylate (MMA) to synthesize smectic clay/PMMA nanocomposites with higher storage modulus and T_g than those without using clay.[16,17] Salahuddin et al., prepared MMT (claytone)/PMMA with improved linear dimensional stability, which might find applications in dentistry.[18] Zhu et al. used three different ammonium salts to modify the clay and then carried out bulk polymerization to form clay/PMMA nanocomposites that exhibited higher thermal decomposition temperatures and lower peak heat release rate (Cone calorimetry) than pristine PMMA.[19] Tabtiang et al. prepared clay/PMMA composites both by solution polymerization of MMA and by melt intercalation of PMMA. The former method was reported to yield a product with higher homogeneity, T_g, and storage modulus.[14]

In spite of the work of Tabtiang et al., the current research further investigates in detail the factors that affect the properties of composite formed by the melt blending process. It is interesting to find that the commonly overlooked processing parameters, such as blending temperature, blending time, and post hot-pressing treatment, had a strong effect on the level of exfoliation and dispersion of the clay, as revealed by XRD studies. Thermal properties of the composites were examined using TGA and DSC analyses. Based on the clay/PMMA nanocomposite, a new type of bone cement was prepared using a formulation typical for commercial bone cement products.[24–27] The impact strength of the synthesized bone cements were determined and compared with that of the surgical Simplex P. Moreover, human osteoblast-like MG63 cells were selected to evaluate the cell biocompatibility of the prepared bone cements.[28,29]

Experimental Part

Material

Montmorillonite (MMT clay) with a cation exchange capacity of 77 meq per 100 g was supplied free of charge by Pai Kong Ceramic Materials Corp., Taiwan. Octadecylammonium (Acros, mp = 50–52 °C, bp = 232 °C) was used to modify the clay by an ion exchange procedure described below. PMMA (CM-205, Chi Mei Corp., Taiwan, $\overline{M}_w = 85\,000$–$90\,000$) was blended with the modified clay to form organic-inorganic composites. Other ingredients for preparing bone cement, including MMA, 2-hydroxyethyl methacrylate (HEMA), barium sulfate, and benzoylperoxide were purchased from Acros. These chemicals were at least of reagent grade and were used as received.

Methods

Clay/PMMA Nanocomposite Formation and Characterization

An ion exchange process was used to prepare the organic-compatible MMT clay. In a typical experiment, 20 g of clay was added to 1 l of distilled water at 80 °C. The mixture was agitated for 1 h to obtain a uniform dispersion. Meanwhile, 12.45 g of octadecylammonium (i.e., three times the CEC value of clay) was dissolved in a 600 ml hydrochloric acid solution (0.63 M) in which protonation of the amine groups took place to form quaternary ammonium ions, $CH_3(CH_2)_{17}NH_3^+$. This solution was mixed with the as-prepared clay/water dispersion medium at 80 °C for 2 h, during which sodium ions in the clay underwent ionic exchange with the quaternary ammonium ions. A series of washing and filtrating (with distilled water) steps were conducted to remove unwanted ionic species and impurities so as to obtain the organo-modified clay. Silver nitrate was used to test whether the filtrate (essentially clay) still contained residual chloride ions. The obtained wet organo-modified clay was dried in an oven at 50 °C.

The clay-PMMA composites were prepared by the well-known melt intercalation method. A specific amount of dried organo-clay was blended with PMMA at 200 °C at 60 rpm in a mixer (Brabender, plasti-corder PL-2100-5) for either 10 or 20 min. The formed composite was ground into powder and then hot pressed (100 kg · cm^{-2}) to obtain film-type samples for subsequent tests. In a number of cases, different pressing temperatures (180 and 200 °C) and pressing times (60, 120, and 180 min) were undertaken to study their effects on the expansion of the silicate's inter-lamellar space (termed d-space hereinafter) and the physical properties of the composites. The preparation conditions for various composites are summarized in Table 1 and 2 and the formed composites were characterized by the following methods:

(1) XRD (Bruker, D8 Advanced) was used to determine the width of the intercalated inter-lamellar distance. The X-ray radiation source had a wavelength of 1.54 Å (copper $K_{\alpha 1}$, Ni filter) at 30 kV and 30 mA. The width of the aperture slit was 0.1 mm, and the scanning rate was 0.01 degrees per s over the range of $0.5^\circ < 2\theta < 10^\circ$.

Table 1. Properties of OA-clay/PMMA composite materials (for TGA and XRD experiments, powder samples were used).

Code	Clay content	Blending time[a)]	T_g		T_d
	%	min	°C		°C
			1st Run	2nd Run	
M1A	1	10	119	119	339
M3A	3	10	119	119	339
M5A	5	10	119	119	339
M7A	7	10	119	117	343
M9A	9	10	118	117	343
M1B	1	20	119	117	340
M3B	3	20	117	116	343
M5B	5	20	117	116	348
M7B	7	20	116	116	356
M9B	9	20	115	116	367

[a)] Blending temperature was 200 °C for all samples.

(2) The morphology and the lamellar structure of the composites were observed by transmission electron microscope (TEM, JEOL, JEM-1200EXII, Japan). The composite powder was dispersed in ethanol in an ultrasonic bath. A drop of dilute liquid sample was placed on a standard 300-mesh grid. Ethanol was removed under evacuation, and the dried sample left on the grid was observed at magnifications of 50 000–400 000× at an acceleration voltage of 75–80 kV.

(3) The thermal decomposition behavior and glass transition temperature of the composites were examined using a thermal analyzer (Hi-Res TGA 2950, TA Instrument, USA) and a differential scanning calorimeter (DSC, TA Instrument, USA), respectively. The heating rates were 10 °C · min^{-1} for TGA and 20 °C · min^{-1} for DSC. The scanning ranges were 25–600 and 25–180 °C, respectively, for these instruments. All experiments were carried out under nitrogen atmosphere.

Bone Cement Preparation and Impact Strength Test

A series of bone cements were prepared with recipes modified from the surgical bone cement, Simplex P. The detailed compositions of various ingredients for different samples are listed in Table 3. The weight ratio of solid to liquid components was fixed at 1.75. Both intercalated and non-intercalated clay/PMMA composites were employed to test the effects thereof. The liquid and solid components were mixed mechanically and then poured into a mold until a hard bone cement was formed, which took about 1–2 min. Tests of the impact strengths of the bone cements were performed at room temperature using an Izod-type impact instrument. The elevation angle of the striker was set to 150°. The dimensions of the samples were 25 × 9 × 2 mm. The impact moment at strike (product of weight of the striker and length of the pendulum) was 16.63 kgf · cm^{-1}. For all samples, tests were repeated three times and the average values were reported.

Table 2. Properties of OA-clay/PMMA composites after heat treatment.

Code	Powder source	Clay content	Press temperature	Press time	T_g	T_d
		%	°C	h	°C	°C
P5A1	M5A	5	180	1	117	349
P5A2	M5A	5	180	2	117	349
P5A3	M5A	5	180	3	115	351
P5B1	M5A	5	200	1	118	360
P5B2	M5A	5	200	2	116	350
P5B3	M5A	5	200	3	117	350
P9A1	M9A	9	180	1	114	343
P9A2	M9A	9	180	2	118	343
P9A3	M9A	9	180	3	117	350
P9B1	M9A	9	200	1	116	349
P9B2	M9A	9	200	2	118	350
P9B3	M9A	9	200	3	114	350

Cell Culture

MG63 cells (American Type Culture Collection, Rockville, MD, USA) were selected to evaluate cell biocompatibility of the prepared bone cements. The culture medium used was Dulbecco's modified Eagle's medium (DMEM) supplemented with 10% fetal calf serum (Gibco-BRL Life Technologies, Paisley, UK) and antibiotic/antimycotic (penicillin G sodium 100 U · ml^{-1}, streptomycin 100 μg · ml^{-1}, amphotericin B 0.25 μg · ml^{-1}, Gibco-BRL Life Technologies, Paisley, UK). MG63 cell line was trypsinized using 0.1% trypsin and 0.1% ethylenediaminetetraacetic acid for 5 min, centrifuged at 400 *g* for 5 min, and resuspended in the medium. For determination of the cell adhesion and cell growth, the prepared bone cements with 15 mm diameter were placed in 24-welled tissue culture polystyrene (TCPS) plates (Corning, Action, MA, USA). Samples were sterilized in 70% ethanol overnight and rinsed extensively with phosphate buffered saline (PBS), followed by treatment under ultraviolet light overnight. Subsequently, 1 ml medium of cell suspension at a concentration of 8×10^4 cells per ml was added to each well and maintained in a humidified atmosphere with 5% CO_2 at 37 °C for a predetermined period.

The viability of MG63 cells on the bone cements was determined by MTT assay [3-(4,5-dimethylthiazol-2-yl)-2, 5-diphenyl tetrazolium bromide]. The method of Mosmann was modified and used in this study.[30] MTT (M-2128, Sigma, St. Louis, MO, USA) was prepared as a 2 mg · ml^{-1} stock solution in PBS, sterilized by Millipore filtration, and kept in dark. The MTT solution of 100 μl was added to each well. After 3 h incubation at 37 °C, 200 μl of dimethyl sulfoxide (Nacalai Tesque, Kyoto, Japan) was added to dissolve the formazan crystals. To achieve complete dissolution, the mixture was jogged for about 15 min on a shaker. The optical density of the formazan solution was read on an ELISA plate reader (ELx 800, BIO-TEK, Winooski, VT, USA) at 570 nm. The absorbance was proportional to the number of cells attached to the bone cement surface.[30]

Results and Discussion

Modification of Montmorillonite

Montmorillonite clay was intercalated by octadecylammonium to form organophilic clay (termed OA-clay herein-

Table 3. Compositions and impact strength of bone cements.

Code	Liquid component		Solid powder component				Impact strength
	MMA	DMPT	PMMA	PMMA/clay	$BaSO_4$	BPO	$kJ \cdot m^{-2}$
	%	%	%	%	%	%	
A	97.5	2.5	90	0	10	<1	3.20
B	97.5	2.5	0	90[a)]	10	<1	3.35
C	97.5	2.5	0	90[b)]	10	<1	3.35
D	97.5	2.5	0	90 (M5A)	10	<1	4.70
E	97.5	2.5	0	90 (M9A)	10	<1	5.01
F	97.5	2.5	0	90 (M5B)	10	<1	5.32
G	97.5	2.5	0	90 (M9B)	10	<1	5.47

[a)] Unmodified clay/PMMA = 5/95, blending time= 10 min.
[b)] Unmodified clay/PMMA= 9/91, blending time= 10 min.

after). Its X-ray diffraction pattern is shown in Figure 1 along with the pristine unmodified clay. For the unmodified clay, curve A indicates a diffraction peak at $2\theta = 6.9^\circ$, corresponding to an inter-lamellar distance of 1.28 nm, as calculated from Bragg's law ($2d \sin\theta = n\lambda$). After ion exchange, the *d*-space of the clay increased considerably. As is obvious from curve B, the major diffraction peak shifts to $2\theta = 2.8^\circ$ or $d = 3.1$ nm. A minor peak (5.6°) and a small hump (8.5°) are also observed, which correspond to $n = 2$ and 3 cases in the Bragg's law. Thus, it is very likely that octadecylammonium has entered and expanded the *d*-space of the clay by means of ion exchange with the cations absorbed on the lamellae surface.

Formation of Clay/PMMA Nanocomposite

PMMA was blended at 200 °C for various periods with both pristine and OA-clays to prepare composite materials. The XRD diffractograms of the formed composites are demonstrated in Figure 2 and 3. Samples in powder form were used for all the XRD scans. Figure 2 depicts the cases for which 1–9% of OA-clay was blended with PMMA for a period of 10 min (cf., M1A–M9A in Table 1). It can be seen that when the OA-clay contents were low, such as M1A and M3A, diffraction peaks were barely identifiable over the scanning range of $0.5^\circ < 2\theta < 10^\circ$. This is because the clay contents of these samples were too low to generate enough diffraction intensity by coherent reflection of the ordered silica plates. Diffraction patterns M5A, M7A, and M9A, are for samples containing 5, 7, and 9% OA-clay, respectively. The major diffraction peaks are all located at $2\theta = 2.3^\circ$ corresponding to a *d*-space of 3.8 nm. Apparently, PMMA has been melt intercalated into the lamellae space of the OA-clay, resulting in expansion of the *d*-space by more than 25%, as compared with OA-clay. In contrast, attempts made to insert PMMA into unmodified clay by blending under the same conditions turned out to be futile; the XRD patterns of the formed blends are shown in Figure 3. Except for the

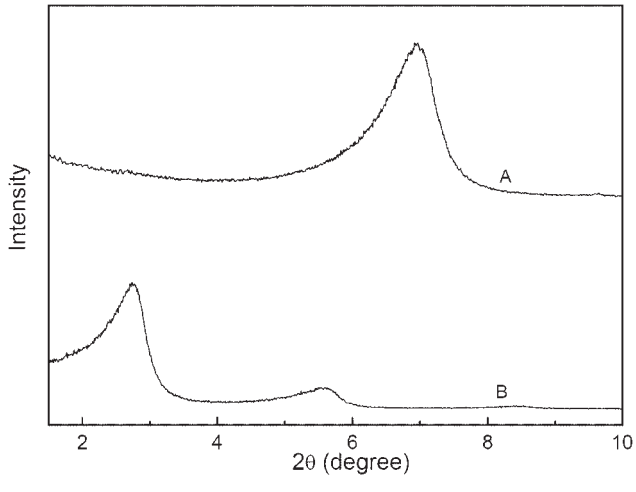

Figure 1. XRD patterns of unmodified (curve A) and organo-modified MMT (curve B).

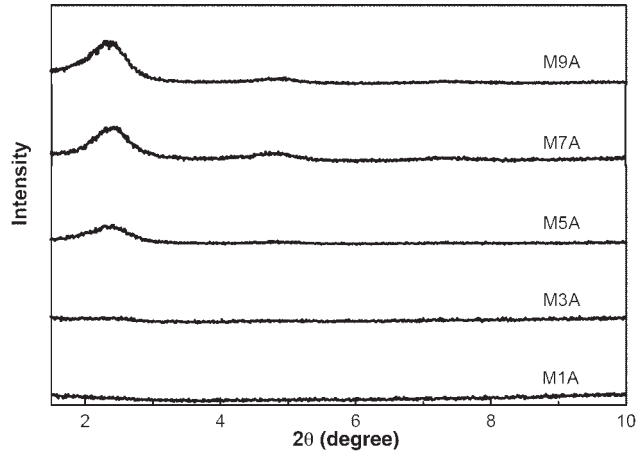

Figure 2. XRD patterns of OA-clay/PMMA powder samples with different OA-clay contents. The blending time was 10 min (cf. Table 1).

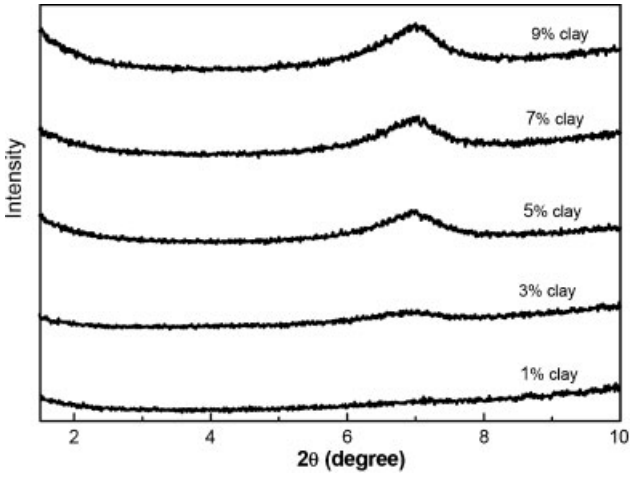

Figure 3. XRD patterns of unmodified clay/PMMA samples with different clay contents. Blending time = 10 min and blending temperature = 200 °C.

pattern with only 1% clay, all others exhibit a peak at $2\theta = 6.9^\circ$, which is exactly the coherent diffraction of the unmodified clay. It appears that the hydrophilic character of the unmodified clay has impeded the entrance of PMMA that was relatively hydrophobic in nature. Also, because the *d*-space of the unmodified clay was very small (1.28 nm) it was difficult for the polymer chain to migrate into it even at an elevated temperature. This suggests that octadecylammonium plays two important roles: on one hand it increases the compatibility between clay and PMMA, and on the other hand it opens up the slits between the lamellae.

In Figure 4, TEM images of a typical powder sample (M5A, Table 1) are shown. From Figure 4(a), stacks of silica lamellae are observed to disperse in the PMMA matrix (cf. dark or deep gray elongated bands). At this magnification, the thinnest identifiable band is ca. 10 nm. Some bands are very wide, e.g., 50 nm, in which alternating dark and light sub-bands are distinguishable. Figure 4(b) shows the high magnification image of a lamella, the width of which is measured to be ca. 4 nm, consistent with the inter-lamellar distance obtained by XRD.

The effect of blending time on the expansion of *d*-space of OA-clay has been investigated and the results are shown in Figure 5. The blending time for all the samples in this figure was 20 min and the OA-clay contents were 1–9%. Patterns M1B, M3B, and M5B (cf. Table 1) are rather flat without appreciable peaks over the scanning range, whereas curves M7B and M9B show very small humps at $2\theta = 2.3$ and 4.6°. Compared with Figure 2, it is clear that increase of the blending time from 10 to 20 min has resulted in pronounced exfoliation of the lamellae. As is obvious, in order to expand the lamellae (≈3 nm wide for OA-clay), a polymer chain has to take a suitable conformation and migrate gradually into the *d*-space. By increasing the blending time, the diffusional flux of PMMA could be

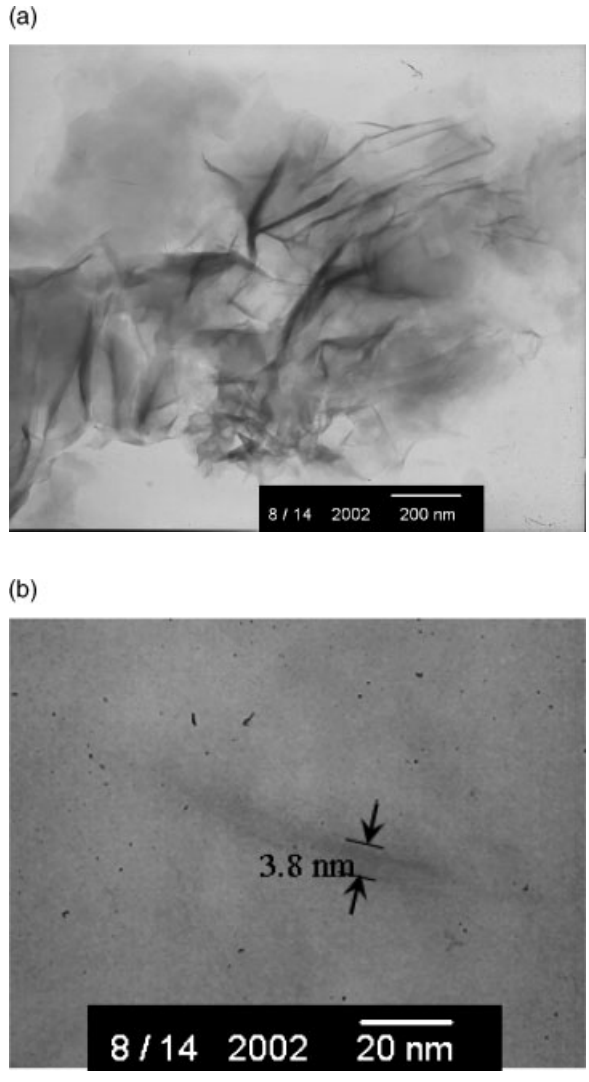

Figure 4. TEM images of an OA-clay/PMMA composite, M5A.

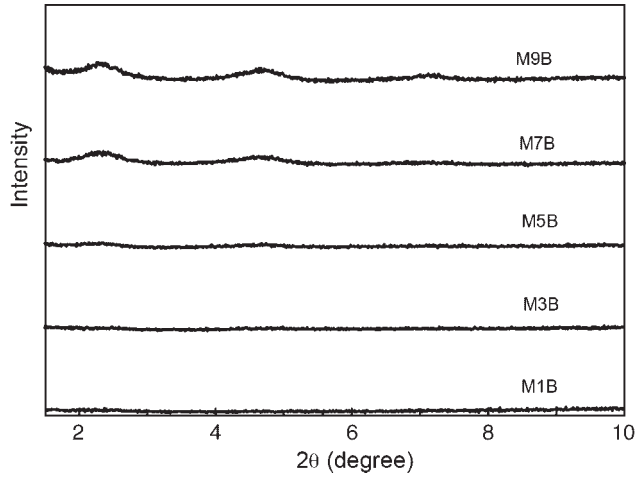

Figure 5. XRD patterns of OA-clay/PMMA powder samples with different OA-clay contents. The blending time was 20 min (cf. Table 1).

increased. Also, exfoliation actually implies the separation of lamellae by entangled polymer chains, which can be greatly facilitated by the shearing force of the blending shaft at 60 rpm. Figure 5 indicates that 20 min is long enough to completely separate the lamellae space of the composite sample with clay content up to 5%. However, for higher clay contents, some small amount of intercalation (ca. 3.4 nm, *d*-space) was still in evidence. It may be interesting to further increase the blending time to yield higher degree of exfoliation; however, this might be at the risk of degradation of some small PMMA chains, and lead to a downgrade of the thermal and mechanical properties.

Various composite powders (Table 1) were hot pressed into dense films for XRD and mechanical tests. The pressing time and pressing temperature were the variables under investigation. In Figure 6, XRD patterns are shown for samples P9A1, P9A2, and P9A3 (cf. Table 2) that were prepared by hot-pressing composite M9A at 180 °C for 1, 2, and 3 h, respectively. It can be seen that the intensities of the diffraction peaks decrease progressively with increasing pressing time; e.g., the intensity of P9A3 is only ca. 40% that of P9A1. This suggests that PMMA continues to expand the silica lamellae during the course of the hot-pressing process. Obviously, it is advantageous to have a prolonged pressing time during which more PMMA chains can migrate into the *d*-space and separate the lamellae. As the pressing temperature was raised to 200 °C, the efficiency of intercalation or exfoliation increased as well, which is also demonstrated in Figure 6. For sample P9B1, which has been hot pressed for 1 h, the X-ray diffraction intensity was comparable with that of P9A2 (2 h at 180 °C). That is, at a higher temperature, it took less time to have similar level of exfoliation. This is associated with the fact that at higher temperature, the viscosity of the composite is lower and the mobility of the polymer chain is higher; thereby better homogenization of PMMA and OA-clay is achieved. It is interesting to notice that after pressing at 200 °C for 3 h, nearly complete exfoliation was attained even for sample P9B3 whose clay content was as high as 9 wt.-%.

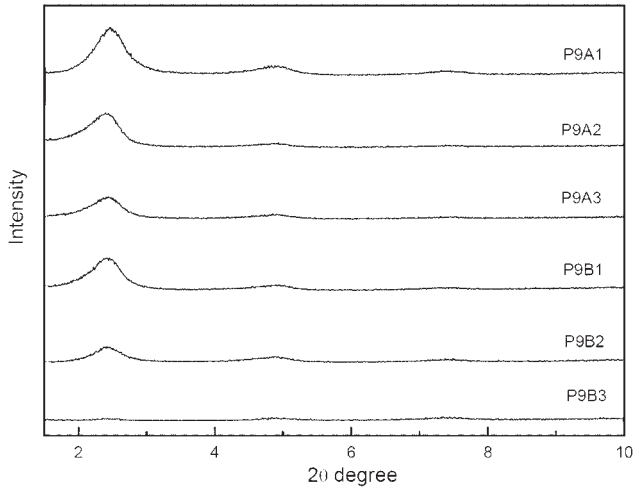

Figure 6. XRD patterns of composite samples prepared by hot pressing M9A at 180 and 200 °C for different times (cf. Table 2).

Thermal Analysis

As discussed above OA-clay can be uniformly dispersed in the polymer matrix in the form of expanded or widely separated lamellae, depending on the process conditions. These nanocomposites demonstrated improved thermal stability, as studied by TGA analysis. Several representative thermograms are presented in Figure 7, and the measured thermal degradation temperatures (T_d at 90%) of all samples are summarized in Table 1 and 2. Figure 7(a) and (b) show the thermograms of pure PMMA and powder samples with different OA-clay contents (1–9 wt.-%) that have been blended for 10 and 20 min, respectively. For all composites, the T_d were higher than that of pure PMMA

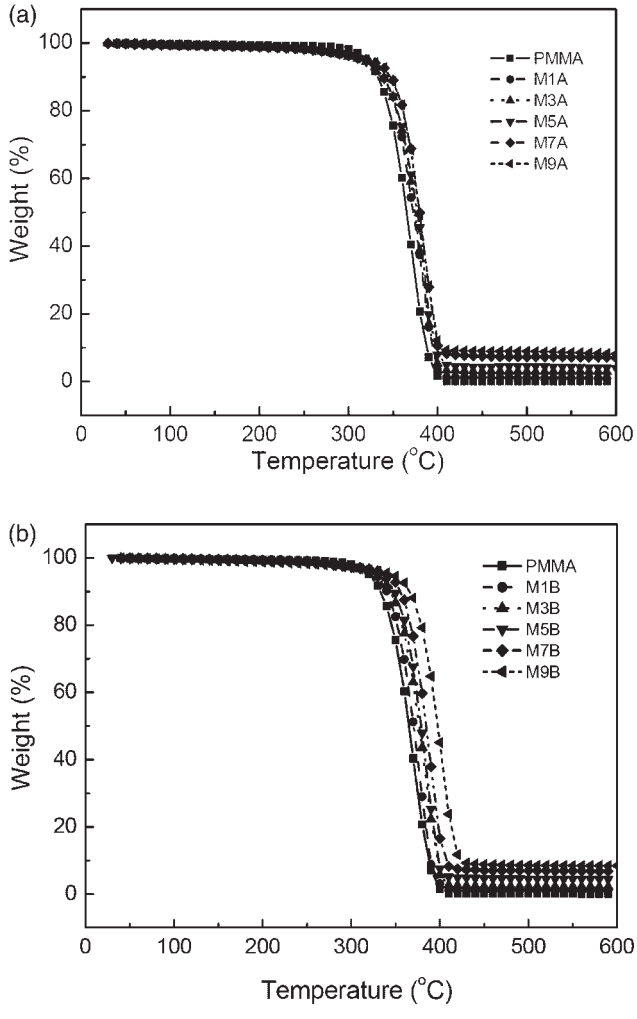

Figure 7. TGA thermograms of pure PMMA and composite powder samples with different weight percent of OA-clay for blending times of (a) 10 min and (b) 20 min.

(332 °C) and they tended to increase with increasing OA-clay content, yet pronounced increase was not observed until 5% or more OA-clay was added. It appears that in these nanocomposites, PMMA chains were strongly bound to the OA-clay either through intercalation or exfoliation of the lamellae. Thus, its thermal stability was improved and its thermal degradation was effectively postponed. For instance, the T_d of sample M9B reached up to 367 °C, being 35 °C higher than that of pure PMMA. The data in Figure 7(b) and Table 1 also indicate that composites prepared after being blended for 20 min are more resistant against thermal decomposition than those with a blending time of 10 min, which is consistent with the XRD results shown previously. As the degree of mixing in the 20 min case became higher, more extensive interfacial contacts and thus stronger interactions between PMMA and clay were there in these samples. However, it is noteworthy that attempts made to improve the thermal stability by blending unmodified clay with PMMA were futile. In fact, T_d values of samples with different amounts of unmodified clay were nearly the same as that of pure PMMA. Apparently, this was due to the poor compatibility between the organic and inorganic phases such that the two components acted independently during the thermal degradation experiments.

For composites that have been blended for 10 min and then hot pressed (cf. Table 2), their T_d was in the range of 340–360 °C, much higher than those of pure PMMA and the corresponding non-pressed samples, i.e., M5A (339 °C) and M9A (343 °C). However, the thermal stability of these samples does not increase accordingly with increasing clay content, hot-pressing temperature, or hot-pressing time. Despite several cases, there seems to be an ultimate T_d value approaching 350 °C for most samples. In other words, although the XRD patterns suggest a higher level of exfoliation and mixing for composites blended at a higher temperature for a longer time, this effect does not entirely reflect on the thermal behavior. It is suspected that some of the PMMA have undergone degradation during the hot-pressing process, which counteracts the improvements of thermal stability derived from intercalation and/or exfoliation with OA-clay. This however requires further research to draw a solid conclusion.

The glass transition temperatures (T_g) of pure PMMA and various composites were measured using DSC. In Figure 8, some typical DSC thermograms at the scanning rate of 20 °C · min^{-1} are presented. The samples are pure PMMA, unmodified clay/PMMA (5% clay), and composites containing different amounts of OA-clay that have been blended for 10 min. The T_g (identified as the mid-point of transition) of these samples and other composites are all collected in Table 1 and 2. It can be seen that pure PMMA has a T_g of 111 °C, which is 8 °C lower than that of the unmodified clay/PMMA composite, indicating that even unmodified clay can still hinder the movement of polymer chains through some interfacial contacts. It is interesting,

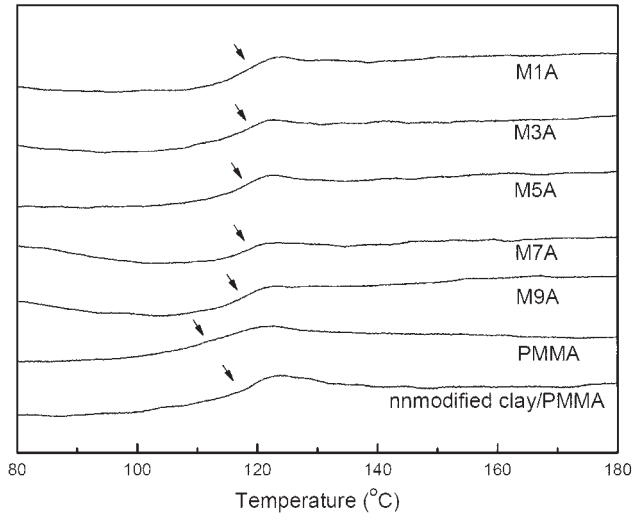

Figure 8. DSC thermograms of pure PMMA and composite samples with different weight percent of clay (cf. Table 1).

however, to find that the T_g does not correlate with the OA-clay content, the blending time, or the blending temperature. The T_g of all composites fall largely within a small range of 114–119 °C. Again, the partial degradation of the polymer during the prolonged hot-pressing process is considered to be the cause of such phenomenon.

Impact Strengths of Bone Cements

Impact strengths of the bone cements prepared by different solid and liquid formulae are summarized in Table 3. Cement A had a composition similar to that of commercial Simplex P and thus served as a reference for comparison. Cements B–G had the same liquid and solid compositions

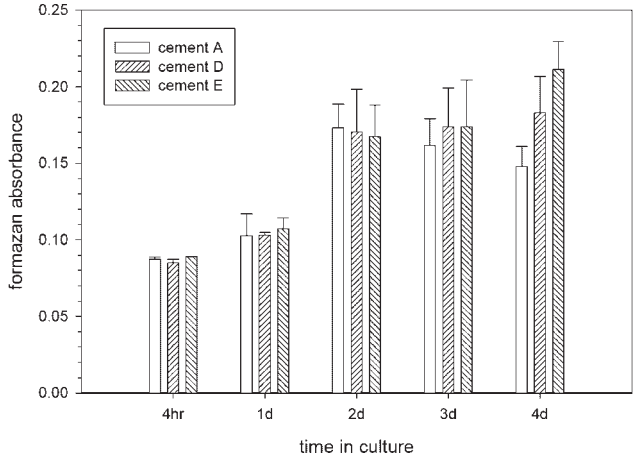

Figure 9. MTT assay. Formazan absorbance of MG63 cells attached to three types of bone cements A, D, and E (cf. Table 3) throughout 4 d of culture. Data are presented as the mean ± standard deviation ($n = 4$).

as cement "A," except that PMMA was replaced by different clay/PMMA composites. When unmodified clay/PMMA was employed (i.e., cements B and C), there was only trivial improvement on the impact strength with respect to cement A. In contrast, when OA-clay/PMMA nanocomposites were adopted to prepare cements D–G, the impact strength increased markedly. For example, for the cases of nanocomposites containing 5 and 9% of OA-clay and being blended for 10 min (i.e., D and E), the impact strength increased by 47 and 56%, respectively. For nanocomposites with a longer blending time (F and G), even stronger cements were obtained, which is associated with the uniformity and exfoliation features of the composites. Specifically, the impact strength of cement G is 1.66 times that of cement A. It is interesting to note that the impact strength of this sample is significantly larger than that of Simplex P (3.64 $kJ \cdot m^{-2}$), suggesting that this new type of bone cement has a potential to substitute the present ones.

Cell Culture

The results in Figure 9 depict the MTT conversion of MG63 cells attached to three types of bone cements A, D, and E (cf. Table 3) throughout 4 d of culture. The MTT assay relies on the ability of the viable cells to reduce a water-soluble yellow dye to a water-insoluble purple formazan product, which has important implication for the cell compatibility of the prepared cements.[30] Figure 9 indicates that MG63 cells on all of the tested bone cements were able to convert the MTT into a blue formazan product, regardless of the bone cement composition. For the first 2 d, MTT counts of cells on cement A were comparable to those on cements D and E, indicating that the OA-clay/PMMA nanocomposites did not inhibit the adhesion and growth of MG63 cells. On the third day of culture, cements D and E had slightly higher accumulation of formazan compared with cement A. Furthermore, MTT counts of cells attached to cements D and E were greater than that attached to cement A after 4 d of incubation. This was not a simple adhesion effect on MTT reduction activity for a continued cell culture, since the adhesion results on different cements were almost equal. Therefore, the OA-clay/PMMA nanocomposites could improve cell growth on traditional bone cements, indicating that the bone cement modification procedure used in this study is reliable and the OA-clay/PMMA nanocomposites are favorable for the culture of MG63 cells.

Conclusion

Clay/PMMA nanocomposites were prepared by melt blending of PMMA with MMT clay that has previously been organically modified by octadecylammonium in a cation exchange process. Various formation parameters, such as blending temperature, time, and clay contents, were examined to see their effects on the intercalation/exfoliation efficiency of the clay. It was generally found that increasing the blending temperature or the blending time increased the level of exfoliation and also the homogeneity of the composites produced. Clay contents had a reversed effect: as it was increased, level of exfoliation tended to decrease. However, by applying a post hot-press treatment at 180–200 °C, extensive exfoliation could be realized even for samples containing as much as 9 wt.-% of organically modified clay. The thermal decomposition and glass transition temperatures of the formed composites were determined by TGA and DSC, respectively. The results indicated a significant improvement on thermal stability versus pure PMMA. The highest attainable T_d was 367 °C, being 35 °C higher than conventional unmodified clay/PMMA composite or pure PMMA. A new type of bone cement was prepared, which incorporated OA-clay/PMMA nanocomposites into the formulation. The OA-clay/PMMA nanocomposites not only raised the impact strength of the traditional cement Simplex P but also improved cell growth on the bone cement surface. Therefore, this paper provides a new method to prepare bone cements with stronger impact strength and better cell compatibility intended for orthopedic surgery.

Acknowledgements: The authors wish to express their appreciation to Mr. *Chih-Yao Yang of Tamkang University* for carrying out some of the thermal analysis work. Also, the authors thank the *National Council of Taiwan* for supporting this research (NSC 91-2216-E-032-001).

[1] Y. Kojima, A. Usuki, M. Kawasumi, A. Okada, Y. Fukushima, T. Kurauchi, O. Kamigaito, *J. Mater. Res.* **1993**, *8*, 1185.
[2] E. P. Giannelis, *Adv. Mater.* **1996**, *8*, 29.
[3] R. A. Vaia, K. D. Jandt, E. J. Kramer, E. P. Glannelis, *Chem. Mater.* **1996**, *8*, 2628.
[4] L. Liang, J. Liu, X. Gony, *Langmuir* **2000**, *16*, 9895.
[5] T. Agag, T. Takeichi, *Polymer* **2000**, *41*, 7083.
[6] S. D. Burnside, E. P. Giannelis, *J. Polym. Sci., Part B: Polym. Phys.* **2000**, *38*, 1595.
[7] D. H. Solomon, B. C. Loft, *J. Appl. Polym. Sci.* **1968**, *12*, 1253.
[8] M. P. Eastman, E. Bain, T. L. Porter, *Appl. Clay Sci.* **1999**, *15*, 173.
[9] A. Usuki, A. Koiwai, Y. Kojima, M. Kawasumi, A. Okada, T. Kurauchi, O. Kamigaito, *J. Appl. Polym. Sci.* **1995**, *55*, 119.
[10] X. Liu, Q. Wu, *Eur. Polym. J.* **2002**, *38*, 1383.
[11] R. A. Vaia, B. B. Sauer, O. K. Tse, E. P. Giannelis, *J. Polym. Sci., Part B: Polym. Phys.* **1997**, *35*, 59.
[12] H. L. Tyan, K. H. Wei, T. E. Hsieh, *J. Polym. Sci., Part B: Polym. Phys.* **2000**, *38*, 2873.

[13] X. Kornmann, H. Lindberg, L. A. Berglund, *Polymer* **2001**, *42*, 1303.
[14] A. Tabtiang, S. Lumlong, R. A. Venables, *Eur. Polym. J.* **2000**, *36*, 2559.
[15] J. H. Park, S. C. Jana, *Polymer* **2003**, *44*, 2091.
[16] M. Okamoto, S. Morita, H. Taguchi, Y. H. Kim, T. Kotaka, H. Tateyama, *Polymer* **2000**, *41*, 3887.
[17] M. Okamoto, S. Morita, Y. H. Kim, T. Kotaka, H. Tateyama, *Polymer* **2001**, *42*, 1201.
[18] N. Salahuddin, M. Shehata, *Polymer* **2001**, *42*, 8379.
[19] J. Zhu, B. Start, K. A. Mauritz, C. A. Wilkie, *Polym. Degrad. Stab.* **2002**, *77*, 253.
[20] J. Du, J. Zhu, C. A. Wilkie, J. Wang, *Polym. Degrad. Stab.* **2002**, *77*, 377.
[21] L. Biasci, M. Aglietto, G. Ruggeri, F. Ciardelli, *Polymer* **1994**, *35*, 3296.
[22] J. M. Hwu, G. J. Jiang, Z. M. Gao, W. Xie, W. P. Pan. *J. Appl. Polym. Sci.* **2002**, *83*, 1702.
[23] M. Okamoto, S. Morita, T. Kotaka, *Polymer* **2001**, *42*, 2685.
[24] W. Krause, R. S. Mathis, *J. Biomed. Mater. Res.: Appl. Biomaterials* **1988**, *22*, 37.
[25] S. S. Haas, G. M. Brauer, G. Dickson, J. Washington, *Bone Joint Surg. Am.* **1975**, *57A*, 380.
[26] J. M. Yang, *Biomaterials* **1997**, *18*, 1293.
[27] G. Lewis, S. Mladsi, *Biomaterials* **2000**, *21*, 775.
[28] J. H. Wang, C. W. Wei, H. C. Liu, T. H. Young, *J. Biomed. Mater. Res.* **2003**, *64A*, 606.
[29] H. C. Liu, I. C. Lee, J. H. Wang, S. H. Yang, T. H. Young, *Biomaterials* **2004**, *25*, 4047.
[30] T. Mosmann, *J. Immunol. Methods* **1983**, *65*, 55.